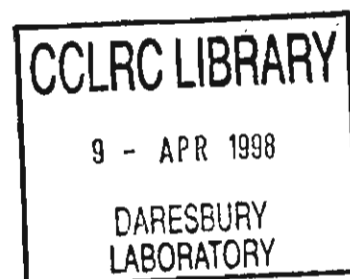




In situ Hydrothermal Synthesis using 13 BM-D at the APS

S Shaw S M Clark Y Wang C M B Henderson C L Cahill J B Parise L Benning
M Rivers and G Shen

March 1998



© Council for the Central Laboratory of the Research Councils 1998

Enquiries about copyright, reproduction and requests for additional copies of this report should be addressed to:

The Central Laboratory of the Research Councils
Chadwick Library
Daresbury Laboratory
Daresbury
Warrington
Cheshire
WA4 4AD
Tel: 01925 603397 Fax: 01925 603195
E-mail library@dl.ac.uk

ISSN 1362-041X

Neither the Council nor The Laboratory accept any responsibility for loss or damage arising from the use of information contained in any of their reports or in any communication about their tests or investigations.

In situ Hydrothermal Synthesis using 13 BM-D at the APS

S. Shaw^{1,2}, S.M. Clark^{2,1}, Y.Wang³, C.M.B. Henderson^{1,2}, C.L. Cahill⁴, J.B. Parise⁴, L. Benning⁵, M. Rivers², G. Shen²

1. Earth Sciences Dept., University of Manchester, Oxford Rd, Manchester; 2. Daresbury Laboratory, Daresbury, Cheshire; 3. GSE-CARS, APS, Argonne National Laboratory, Argonne, Illinois; 4 Dept. Of Chemistry, SUNY - Stony Brook, Stony Brook, NY; 5 Penn State University, Pennsylvania.



Executive Summary

A collaborative team between GSE-CARS at the Advanced photon source (APS), Argonne National Laboratory, a group from the Daresbury Laboratory (SRS) and SUNY at Stony Brook was recently set up to investigate the advantages of performing *in situ* energy dispersive powder diffraction (EDPD) hydrothermal experiments on station 13-BM-D at the APS. The main aim of this project was to develop and further understand the techniques used for this type of research. Experiments of this nature are routinely performed at the SRS but not to 230°C, as the X-ray beam can only penetrate reaction cells capable of operating above this temperature. It was hypothesized that, with the extra benefits of a third generation synchrotron source, i.e. higher X-ray energy and flux, these same experiments could be performed with reaction cells with thicker walls rated for higher temperatures. A secondary aim of the investigation was to develop an on-line injection facility for the reaction cell thus enabling the user to introduce a fluid to the hydrothermal cell held at elevated temperature and hence pressure.

This work was carried out on station 13-BM-D from 15th to 25th January 1998. The experiments are performed by placing the starting mixture into a specially prepared hydrothermal cell. This cell was then heated to the desired temperature, and while the cell is at temperature the reaction mixture was monitored using energy-dispersive powder diffraction (EDPD) with one spectrum being collected every few tens of seconds. These time-resolved diffraction patterns were used to monitor the entire reaction from starting material to end product.

Experiments were performed on two systems, the first being the hydrated calcium silicate system in an attempt to follow the high temperature crystallization of the mineral phases tobermorite, xonotlite and gyrolite. The second was the iron sulphide system in order to observe the formation of pyrite via its various intermediates and to utilize the newly developed injection system.

Results from the hydrated calcium silicate system proved very productive with all 3 phases being successfully formed, as well as transformations from one phase to another being observed. Temperatures up to 315°C were attained and the pressure was successfully contained within the reaction setup. The time-resolved diffraction data

enabled the mechanism and kinetics of the reaction to be observed and many interesting and informative results were obtained (see figure a). The iron sulphide experiments proved more challenging allowing collection of only limited diffraction data, although all aspects of the hydrothermal cell worked perfectly, including the injection system.

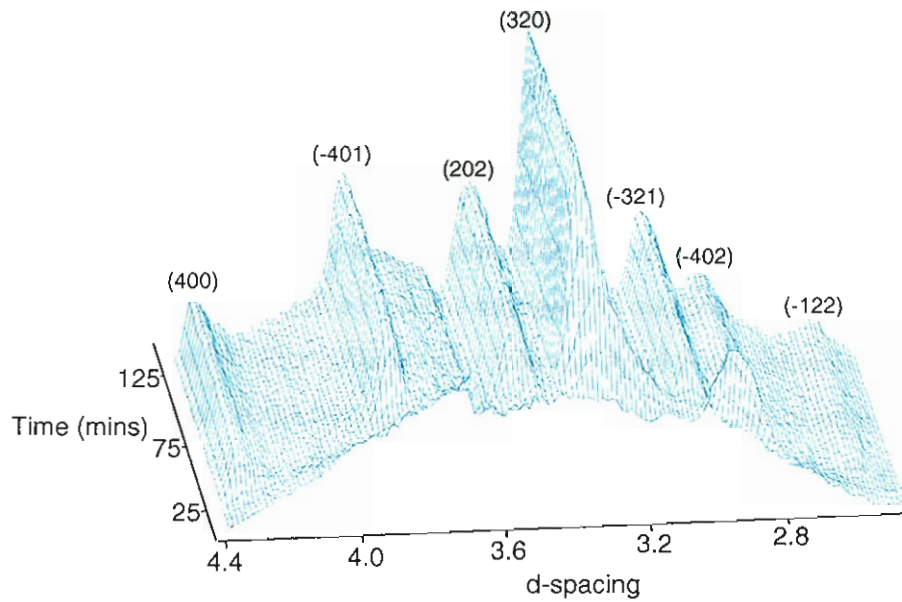


Figure a. Time resolved XRD trace showing the formation of xonotlite at 250°C
Starting composition Ca/Si = 0.833

Introduction

High temperature hydrothermal synthesis is important in both geo-science and materials science [1]. Hydrothermal reactions are usually carried out in sealed steel bombs. Water is included with the reactants inside the bomb and pressure is generated by simply heating the sealed bomb. The saturated vapour pressure generated at a particular temperature can be estimated from steam tables (figure 1). Clearly a bomb with steel walls thick enough to contain the pressure generated must be used so that each bomb will have a maximum safe operating pressure. The conventional method of following the course of a hydrothermal reaction involves quenching the temperature at various times during a reaction and analyzing the quench products *ex-situ*. This always leaves the uncertainty of whether the phases found were actually present in the reaction mixture at pressure and temperature or were only formed on quenching. *In-situ* observation of the reaction is the best way of determining the reaction pathway. High energy X-rays (40-120keV) produced by synchrotron sources are able to penetrate the steel walls of hydrothermal bombs and give usable powder diffraction patterns of the contents in time scales of a few tens of seconds. These patterns can be used to determine which materials

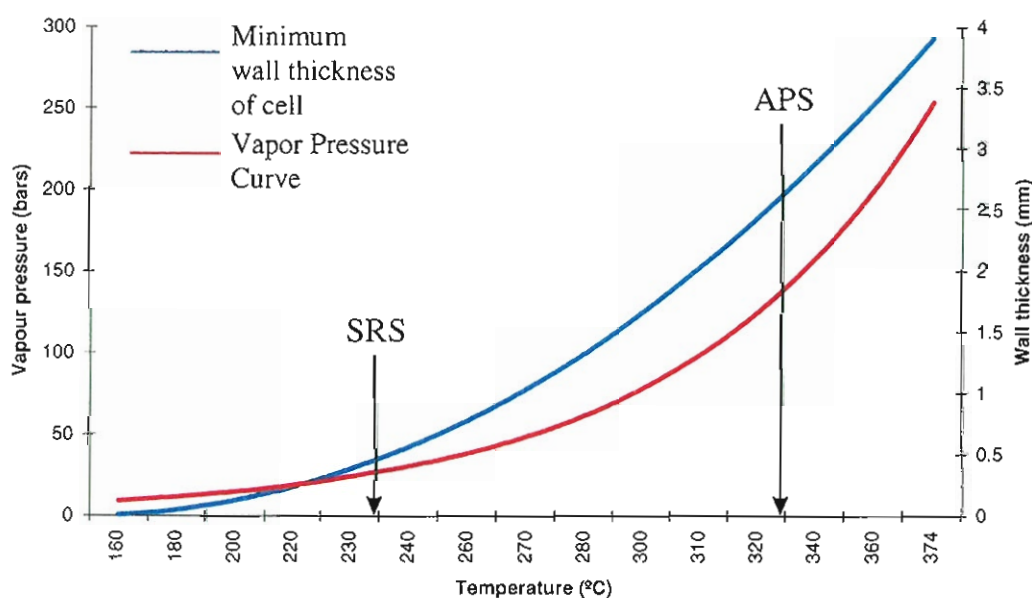


Figure 1. A Comparison of Hydrothermal Temperature achievable at the SRS and APS

are present in the bomb and their relative amounts. The energy-dispersive powder diffraction (EDPD) method is the technique of choice here since the tight pre- and post-sample collimation allows us to exclude any diffraction from the bomb leaving only sample peaks in our pattern. Also, in the EDPD method the whole diffraction pattern is collected simultaneously so we are able to do time-resolved studies of the reactions. A reaction cell suitable for EDPD studies of hydrothermal reactions has been developed and used as part of a collaboration between Daresbury Laboratory and Oxford University [2,3]. This cell has been used on stations 9.7 [4] and 16.4 [5] of the SRS for kinetic studies of for example the formation of microporous solids, zeolite crystallization and clay mineral reactions [6,7,8,9]. The maximum temperature achievable in these experiments has been limited to 230°C by the wall thickness of the bomb which at 0.4mm is the thickest that the X-rays produced by the 6T wiggler magnet on line 16 of the SRS can penetrate and give usable diffraction data in the required time scale.

The APS is a third generation synchrotron source which is a significant improvement on the SRS for these types of experiment. The X-ray energy/flux profile of a bending magnet beam line has at least ten times the flux of a beam line at the Daresbury source and achieves high brightness up to 130 keV. This increased energy range gives improved penetrating power to the X-ray beam, allowing the beam to pass through a reaction cell with walls up to 3mm thick. Therefore hydrothermal experiments at the APS can be done at increased temperatures, up to about 330°C.

It is for this reason that a collaborative team between the GSE-CARS CAT at the APS, SUNY at Stony Brook and Daresbury Laboratory and was set up to utilize the high energy X-rays of the APS for high temperature hydrothermal reaction studies. The experiments were performed on beam line 13BM during January 1998. This is a white beam station with almost identical features to station 16.4 at the SRS making it ideal for this initial investigative study.

Two systems were chosen for this study the first being the formation of the hydrated calcium silicates, tobermorite ($\text{Ca}_5\text{Si}_6\text{O}_{16}(\text{OH})_2 \cdot 14\text{H}_2\text{O}$) gyrolite ($\text{Ca}_{16}\text{Si}_{24}\text{O}_{60}(\text{OH})_8 \cdot 14\text{H}_2\text{O}$) and xonotlite ($\text{Ca}_6\text{Si}_6\text{O}_{17}(\text{OH})_2$). Previous experiments have been completed on these materials at Daresbury, but only within the limited temperature

range discussed above. This system is of particular environmental importance as hydrated calcium silicates and their gel precursors are known to form in hyperalkaline environments. These conditions are analogous to those which are thought to occur around cementitious waste repositories (nuclear and chemical). Therefore the increased understanding of this system should help with understanding the evolution of the host rocks surrounding a waste site over short term geological time scales, giving information on the effects of porosity, permeability and ground water chemistry changes.

The second system is the formation of the iron sulphide, pyrite, in an attempt to characterize the complex reaction pathway which forms this mineral. This is not only important in the context of ore formation, but also environmentally, as iron sulphides are the main active species in the pollution caused by acid mine drainage.

For this second reaction study, another newly developed addition to the on-line hydrothermal technique is utilized. This is an injection system which allows the introduction of liquids into the cell at high temperatures and pressures. Injecting a fluid into a hydrothermal system allows a reaction to be initiated thus allowing, via energy dispersive powder diffraction, the entire reaction sequence to be seen, from unreacted starting material to end product.

Experimental Setup

The investigation was performed on beam line 13 BM, one of the GSE-CARS lines on the APS ring. The beam is produced by a bending magnet yielding a high energy white beam X-ray source. Experiments were taken under in hutch D, 50 m from the tangent point. Prior to entering the hutch, the beam is reduced to an approximately 500μ by 500μ cross section by pre-hutch slits which are motor driven and can be moved externally.

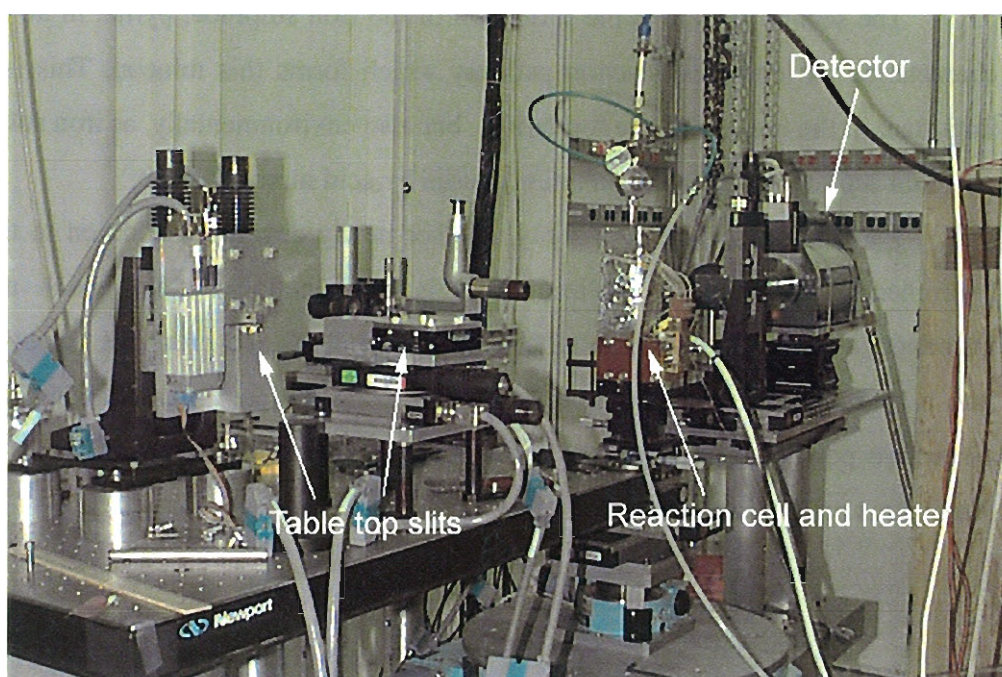


Figure 2. Photograph of experimental setup within hutch 13-BM-D.

The set up within the hutch is basically the same as that used for the diamond anvil experiments (see figures 2 and 3). It consists of two sets of pre-sample table top slits which cut down the size of the incoming X-ray beam. These are simply two pairs of tungsten carbide cubes which are oriented to limit the beam in the horizontal and vertical direction. The position and width of the slits are motor controlled and can be adjusted remotely. It was found that a beam size of 200μ by 50μ was ideal for the experiments being performed giving the required flux without losing significant resolution. Once the incoming beam has passed through the slits it is transmitted through the cell heater unit where it encounters the reaction vessel. The beam is

being performed giving the required flux without losing significant resolution. Once the incoming beam has passed through the slits it is transmitted through the cell heater unit where it encounters the reaction vessel. The beam is diffracted by the contents of the cell to various angles of 2θ , depending on the energy of the particular X-ray photons within the beam. A portion of this diffraction cone is then selected via a 365mm brass collimator with a slit width of approximately 500μ . This ensures that only a very limited range of 2θ is selected in order that only peaks from the sample are detected. The collimated beam is then passed through a final set of adjustable tungsten carbide pre-detector slits where any spurious beam is removed. The detector used is a single element, energy dispersive, solid state, Canberra detector. The collimator and detector are mounted on an arm which can move in 2θ , horizontally about the center of the reaction cell. Any angle of 2θ above 1° (below this value there is a risk of detector damage from the direct beam) can be selected depending on the range of d-spacings being examined during the experiment.

The reaction cell is a modified Anton Parr bar bomb (Part number 4711) with a section of the wall milled down to the required wall thickness (see figure 4). This area is where the X-ray beam passes and the greater the thickness the greater the reduction in X-ray transmission, but the higher the reaction temperature possible (figure 1)

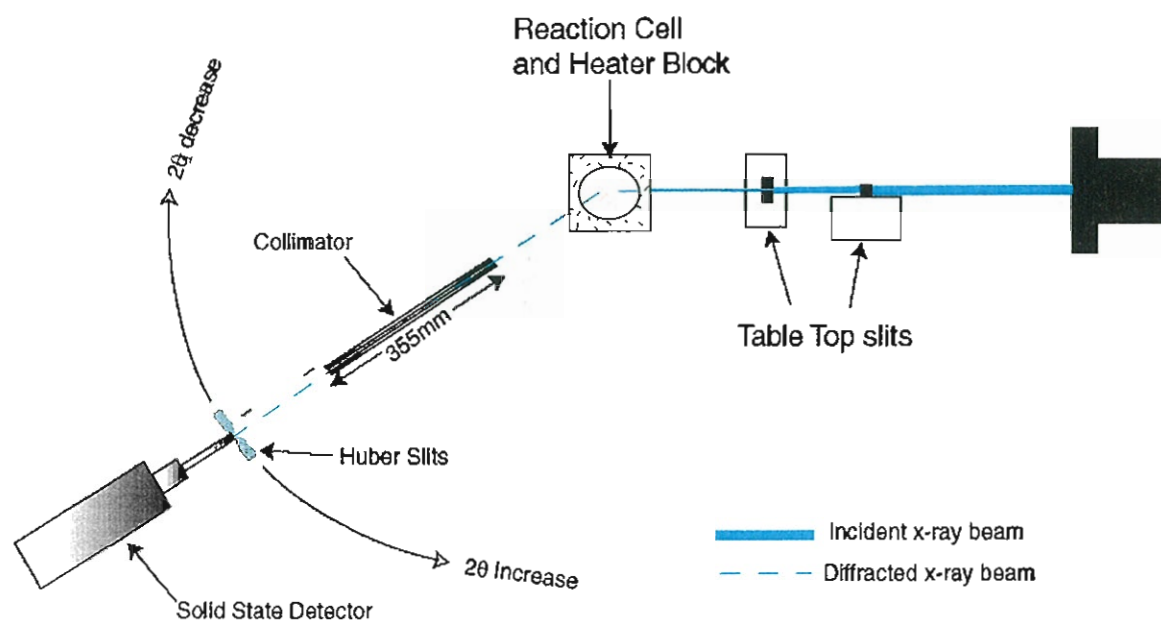


Figure 3. Overhead view of experimental set up within 13BM-D

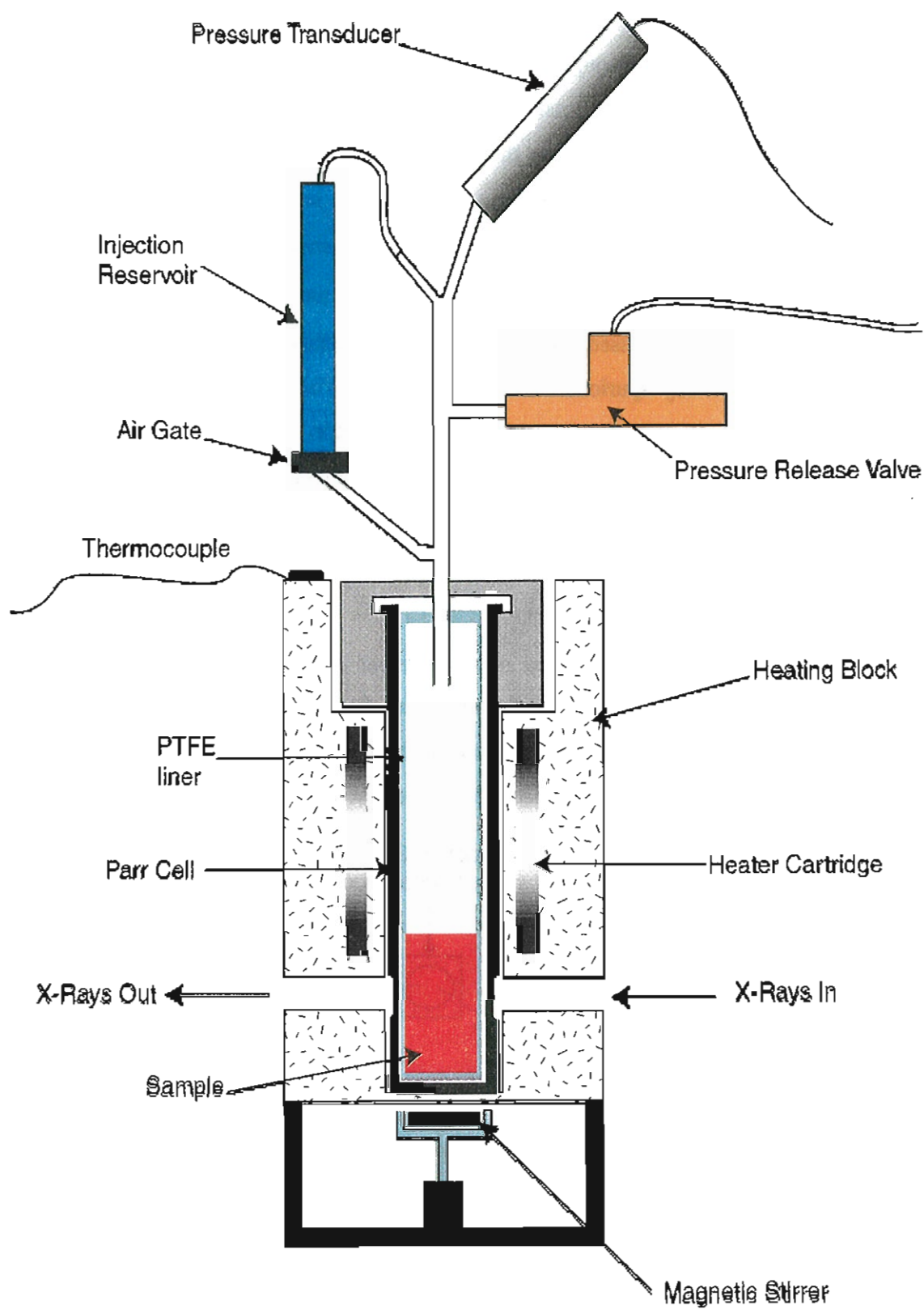


Figure 4. Schematic diagram of on-line hydrothermal reaction cell and heater unit

The cell is open to a head unit at the top, which has a pressure transducer, pressure safety valve and injection system attached. The interior is either PTFE- or copper- lined according to the internal working temperature; at greater than 300°C copper was required as the PTFE breaks down at this temperature. Heating is achieved by placing the Parr cell in an aluminium block which is heated via four resistance cartridge heaters. The heater block unit has incident and exit slits for the in-coming and out-going X-ray beam located in line with the milled-down area of the Parr cell. This allows the X-rays to pass through as little steel as possible. The temperature is controlled remotely using a K-type thermocouple attached to the top of the block.

The injection system consists of a reservoir which is filled with the required solution and blocked at the bottom by a pressure sensitive switch. This pressure-switch can be controlled remotely which allows the user to inject the solution from outside the hutch. The top of the reservoir is attached to the top of the head via a tube, this keeps the solution at the same pressure as the cell interior. When the reservoir gate is opened, the solution flows into the cell under the force of gravity. Stirring can also be achieved in the cell via a micro flea which is rotated by a magnetic stir bar underneath the cell.

According to the temperature of the reaction, a particular cell wall thickness has to be chosen. The thinnest walled bomb allowable is always used to maximize the number X-ray flux reaching the detector. Table 1 shows the different cells, their wall thickness and the maximum temperature and pressure allowed in each.

Table 1. Data on maximum allowable T and P in various different cells.

Cell Wall Thickness (mm)	Maximum Pressure (bars)	Maximum Temperature (°C)
0.4	28	230
1	55	270
2	100	310
3	140	340

Reactants are placed either in the PTFE liner or the solution reservoir prior to heating. For the tobermorite /gyrolite reactions the starting material is a calc-silicate alkoxide gel with the exact stoichiometric compositions of the mineral phase being studied. Saturated calcium hydroxide aqueous solution is then added to the solid in the ratio of five to one. This solution is chosen because it is approximately the composition of the ground water that is expected to form around a cementitious waste site. Once sealed inside, the cell is placed inside the heating block at the required temperature. As the mixture is heated, the gel begins to react and crystalline phases form. The sample is constantly X-rayed during the reaction with a single pattern being taken every 1 to 2 minutes. This gives an comprehensive picture of the crystallization reaction occurring as a function of time. The reactions are performed at different temperatures to compare the kinetics and mechanism of the reaction with temperature.

As well as varying the temperature, the aluminium content of the starting material is also changed, the amount varying from 0% to 15% aluminium substituted for silicon. These experiments were chosen because it has been suggested that aluminium can substitute for silicon in the hydrated calc-silicate lattice and is thought to increase the reaction rate [10,11].

For the iron sulphide reactions an oxygen free solution containing dissolved iron and sulphur was placed inside the reaction vessel and approximately 5ml of sodium hydroxide solution was placed in the injection reservoir. When the iron sulphide solution reaches temperature, approximately 100°C in this case, the sodium hydroxide was released into the iron solution. The rapid increase in pH caused the precipitation of the iron sulphide mineral mackinawite (FeS), which transformed with time to greigite (Fe₃S₄) which then transformed to the final product, pyrite (FeS₂). It was hoped that the entire reaction sequence could be traced through these changes to monitor the mechanism of each stage. The reaction was monitored using time resolved EDPD in the same way as described above.

The XRD data is collected continuously from the solid state detector and divided into the required time-slices by the software. Each individual XRD pattern was saved as a separate file and represents a particular time slice of the reaction. This technique is

especially amenable to kinetic studies as the peak position, areas and the full width at half maximum (FWHM) can be used to define the extent of the reaction, ultimately yielding information on activation energies, orders of reaction and mechanisms.

The remote motor control and time resolved XRD collection were all controlled using IDL software which had been extensively adapted for this set up by Dr Mark Rivers, with user-friendly graphical interfaces for all stages of the experimental procedure including time-resolved data collection, 3 dimensional data plotting and data processing features such as peak fitting. This complete package covers almost all the computational experimental procedures required using the same software package reducing the need for any complex file transfer and data reformatting.

Results

The results of the calc-silicate runs are summarized in table 2. There were 26 runs in total, only the completed runs are listed below. The runs not listed were not completed for reasons such as pressure leaks or wrong run file number assignment during the software set up. Most runs were completed, with only 3 yielding no data.

Among the first set of runs (runs 10,12 and 13) were the gyrolite formation experiments. All produced the desired end phase, gyrolite with no evidence of the higher temperature phase truscottite in any of the runs (see figure 5). The runs were for a maximum of four hours, but no significant changes could be observed after two hours. It could be clearly seen that as the wall thickness of the cells was increased, for higher temperature runs, the count rate was noticeably reduced. Despite this, usable time-resolved data were collected up to 315°C in a 3mm thick walled bomb. This run was the highest temperature attempted in this session and was a complete successes. Although the starting gels for these experiments are produced to be X-ray amorphous, it seems that there was a small amount of crystalline phase in the gel to begin with. The peaks from this material were matched to larnite (Ca_2SiO_4), but were of no real significance as they disappeared in the first few minutes of the reaction.

One problem that was encountered during these experiments were steel diffraction peaks at low d-spacings (1-2 Å). These are produced by diffraction from the hydrothermal cell, but were not a major hindrance as they fell just outside the d-spacing region being observed. These peaks come from having an excessively large diffracting area suggesting that the slit size of the collimator in this case is too large.

The largest set of calc-silicate experiments were carried out on the tobermorite composition gels (runs 14 to 23) with or without aluminium, in an attempt to study the crystallisation of tobermorite and the higher temperature phase xonotlite. These produced noticeably different results as can be seen in table 2 and in figures 6,7,8 and 9. All experiments were completed within 5 hours with the main phase of growth always being within the first 60 minutes. Crystalline tobermorite, xonotlite or a mixture of both were the three end products of the reaction.

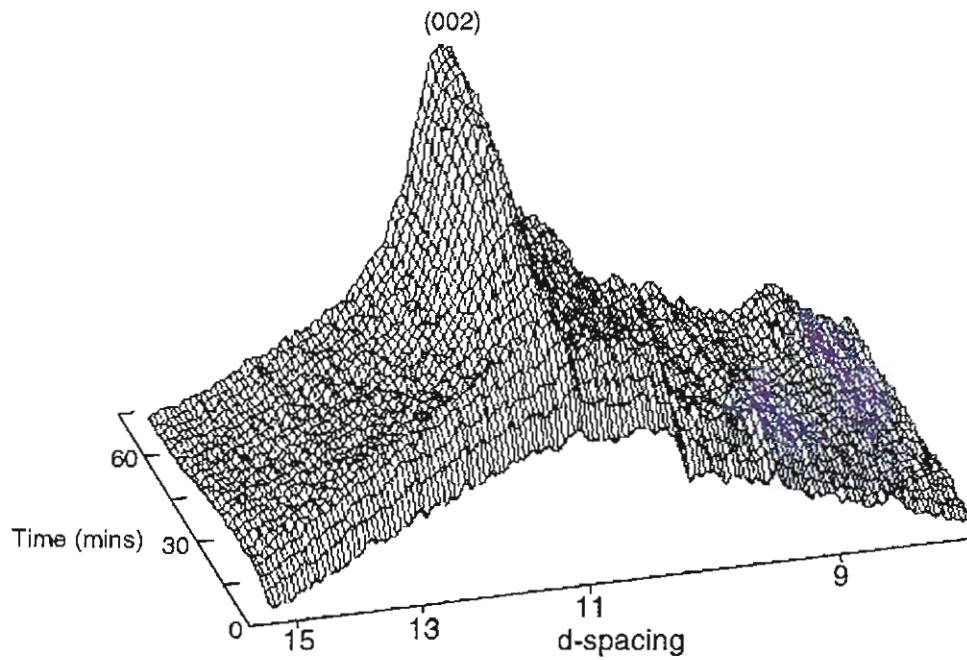


Figure 5. Run13, Time resolved XRD trace showing the formation of gyrolite at 270°C. Starting composition Ca/Si = 0.66.

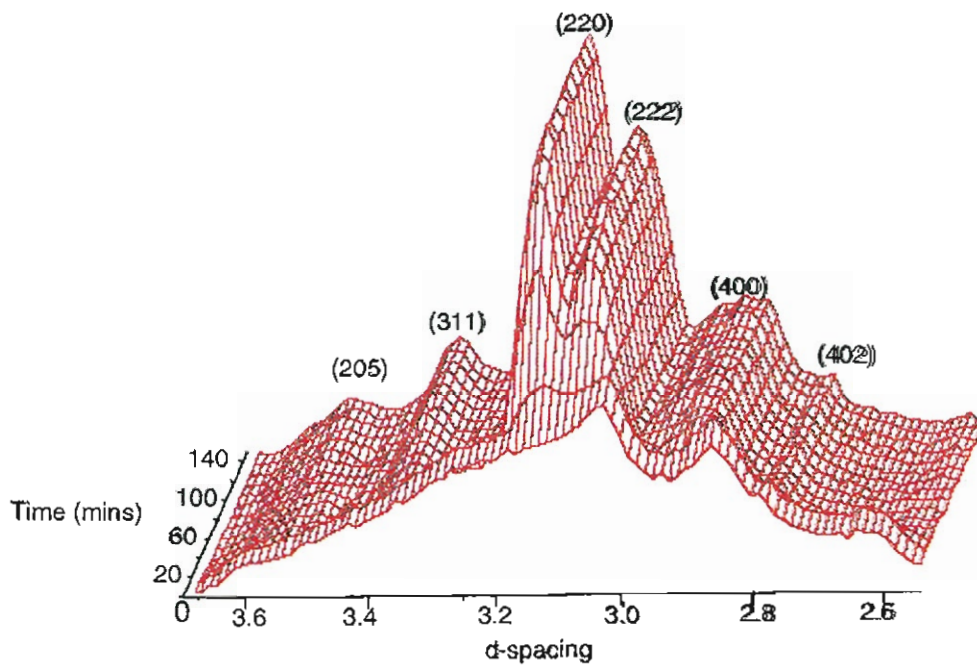


Figure 6. Run19, Time resolved XRD trace showing tobermorite formation at 250°C. Starting composition Ca/Si=0.833.

Table2. Summary of calc-silicate experiments

Run #	Temperature (°C)	Pressure (bars)	Composition of Reagent	Cell wall thickness (mm)	Reagent code	Reaction products
3	250	40.5	tob	1	G55	gyr
4	268	53	tob	1	G48	xon
8	290	72	tob	2	G50	xon,gyr
9	250	40.5	tob	1	G48	gyr
10	267	51.2	gyr	1	G53	gyr
12	316	106.2	gyr	3	G53	gyr
13	263	49.2	gyr	1	G53	gyr
14	266	50.3	Al-tob (10%)	1	G67	tob,xon
15	269	54	Al-tob (5%)	1	G69	xon,(tob)
16	269	54	Al-tob (15%)	1	G68	tob
17	245	36	Al-tob (5%)	1	G69	xon,(tob)
18	246	37	Al-tob (10%)	1	G67	tob
19	245	36	Al-tob (15%)	1	G68	tob
20	290	75	Al-tob (5%)	2	G69	xon
21	290	75	Al-tob (10%)	2	G67	xon
23	288	72	Al-tob (15%)	2	G68	tob,(xon)
24	289	73	tob	2	G47	xon
25	245	36	tob	1	G47	gyr
26	290	75	tob	2	G50	xon

Abbreviations: gyr = gyrolite, tob = tobermorite, xon = xonotlite, Al-tob (x%) = aluminium tobermorite where x = % of Si was substituted by Al.

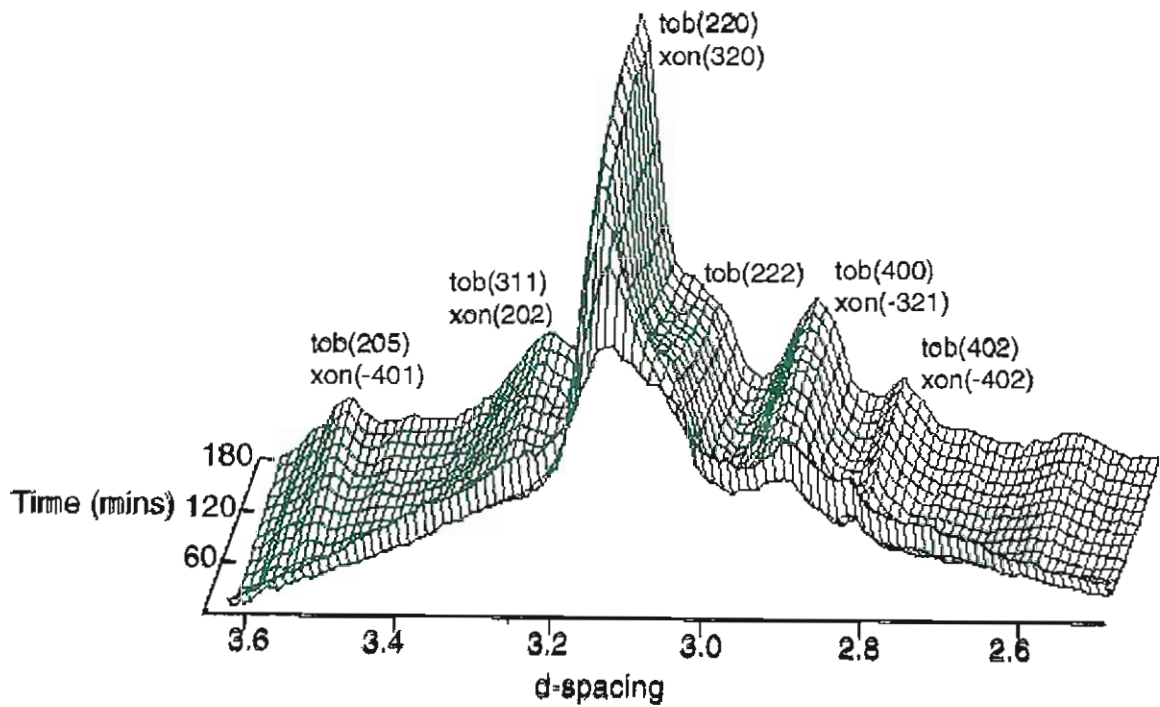


Figure 7. Run17, Time resolved XRD trace showing the formation of a mixed tobermorite/xonotlite product at 250°C. Starting composition Ca/Si=0.833

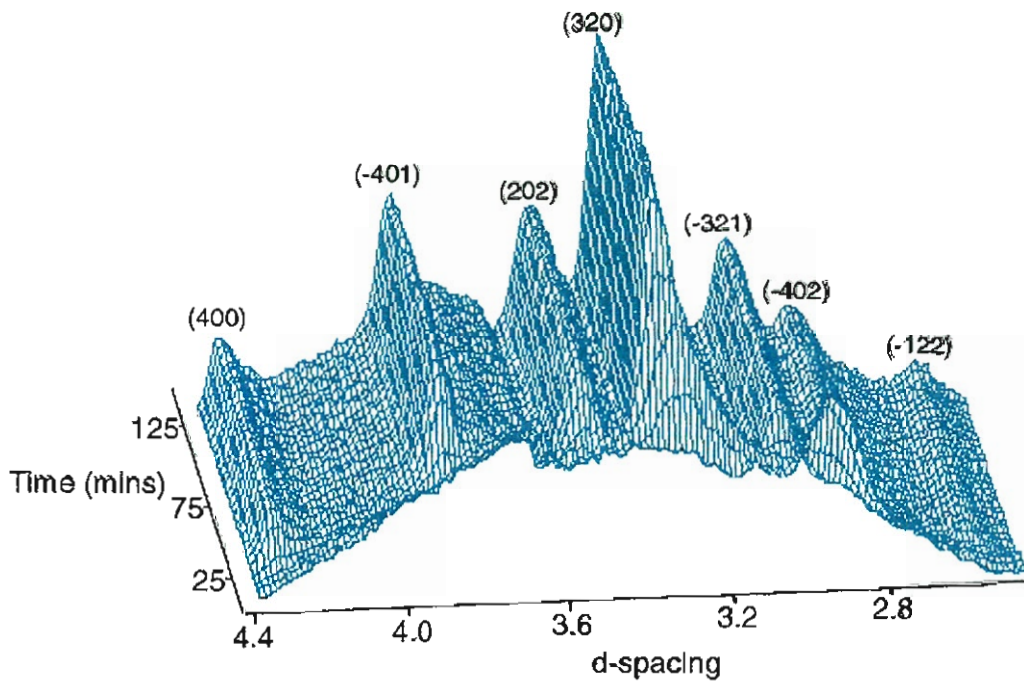


Figure 8. Run4, Time resolved XRD trace showing the formation of xonotlite at 250°C. Starting composition Ca/Si= 0.833.

In all but 2 cases (runs 4 and 26) tobermorite formed first. Note that tobermorite and xonotlite have very similar XRD traces making them difficult to distinguish (see figure 7), the main difference being a peak at 2.98\AA (222) which is uniquely tobermorite and one at 4.21\AA which is only found in xonotlite. Figures 6, 7 and 8 show representative time-resolved data for the three end products. Figure 6 shows the formation of tobermorite in run19; it can be clearly seen that all the peaks for tobermorite in this d-spacing range are present and there is no sign of a reduction in peak intensity towards the end of the reaction which would indicate transformation to another phase. Figure 8 shows the formation of xonotlite in run 4; there is no evidence of tobermorite having formed, i.e. no 222 peak at 2.98\AA , and crystallization occurs quickly within 45 minutes. After this short growth period there is no real change in the trace apart from some peak narrowing as the crystallites increase in size. Figure 7 shows the intermediate between these last two cases in that a mixture of tobermorite and xonotlite is produced. Tobermorite seems to be the first phase to crystallize but as the reaction proceeds the main tobermorite defining peak at 2.98\AA (222) seems to decrease while all the other peaks, which are present in xonotlite, continue to grow. Although the reaction was stopped after three hours it can be seen that the tobermorite peak is still decreasing indicating that, with time, pure xonotlite

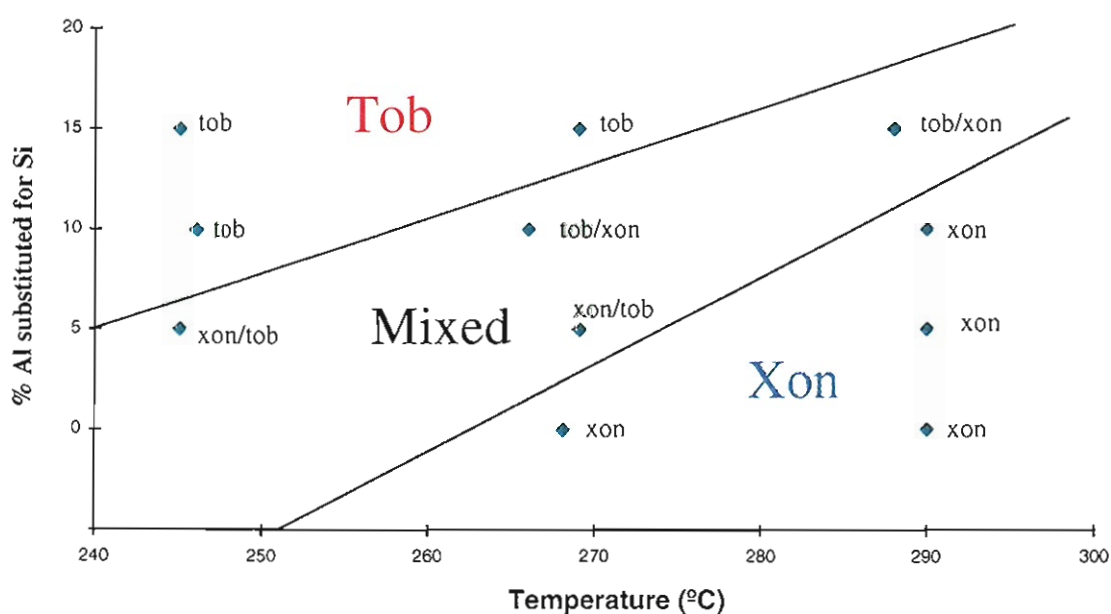


Figure 9. Summary of all tobermorite runs showing the stability field of tobermorite and xonotlite as a function of temperature and Al content

would be produced as the final stable phase.

From these tobermorite composition experiments a clear pattern can be seen when the temperature, composition and reaction product are examined together (see figure 9). In summary it seems that as the aluminium content is increased and temperature decreased tobermorite becomes the more stable phase, and conversely as temperature is increased and aluminium content decreased xonotlite becomes the more stable phase. These are only preliminary observations and until the data has been fully analysed one can not tell if the tobermorite stability is only a feature of reaction kinetics.

Initial data analysis of the time-resolved data has been performed by fitting the diffraction peaks in the data for run 16 only at this stage. The fitted spectra show that the initial phase of growth during the first 60 minutes of the reaction can be characterised by an increase in peak area and reduction in peak width (FWHM). After this period most of the peak features seem to remain relatively constant indicating that the main growth phase is over (see figure 10). From closer examination of the data it can be seen that after this initial growth phase some peaks begin to decrease slightly in intensity (2-3%). This may represent the beginning of a slow transformation from tobermorite to xonotlite or it may

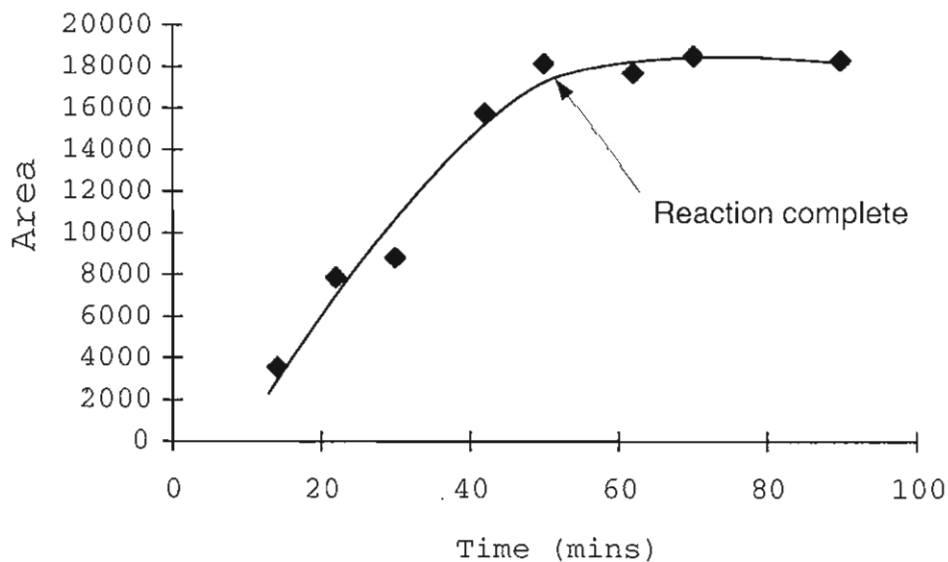


Figure 10. Run16, Tobermorite (222) peak area vs time

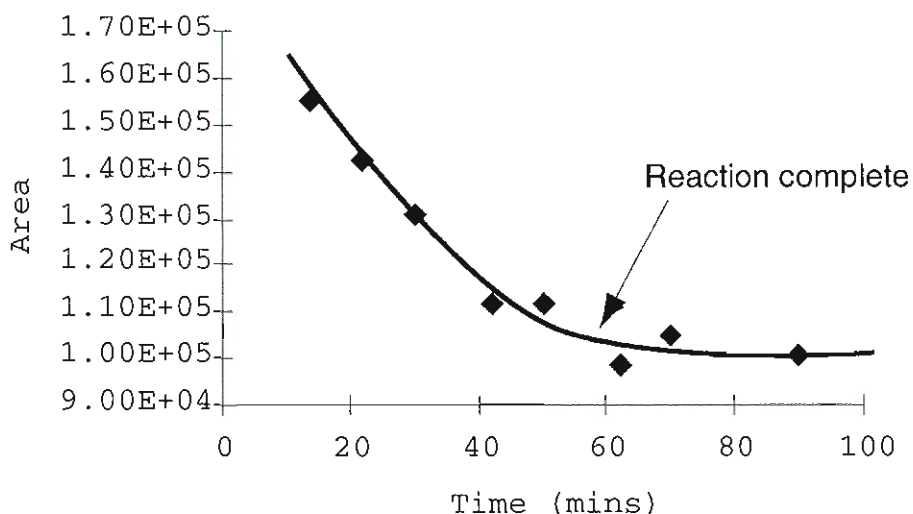


Figure 11. Run16, Background area vs time

be a feature of the beam slowly decaying. Figure 11 shows the background area of the EDPD spectra, caused by scattering from the amorphous gel, as a function of time. It can be seen that this reduces with time as the tobermorite crystallises and the amount of amorphous material is reduced. This agrees with the peak fitting data indicating that the reaction has finished after about one hour.

The iron sulphide experiments proved more difficult than first anticipated. The technique of injecting sodium hydroxide into the 2000 ppm iron sulphide solution worked well with the desired solid being precipitated but no peaks appeared on the XRD trace. This was because the crystalline material was dispersed as a very fine colloid in the solution, with either too little material for the beam to detect or the crystal size being too small. To combat this problem the starting solution concentration was increase to approximately 5000ppm Fe but this had no effect. The final approach was to precipitate a large volume of iron sulphide offline, filter it, then place the resulting paste in the hydrothermal cell before heating to between 100°C and 150°C. Initially this only gave the peaks for mackinawite but with time peaks for greigite and pyrite formed. The entire reaction sequence was not observed but with more time to study this system we are confident that all the problems can be tackled successfully.(For a more in-depth account of these experiments please refer to report by C. Cahill, Feb 1998))

Discussion

In conclusion the collaboration between Daresbury, Manchester University, GSE-CARS and Stony Brook was a great success with all the main goals of the investigation being achieved to a satisfactory level:-

- The maximum temperature of the hydrothermal experiments was increased by almost 100°C compared with the same experiments at the SRS.
- Cells with up to 3mm wall thicknesses were utilized and usable diffraction data was obtained with only 120 second collection times.
- Pressure in the cells was more than double that of previous experiments and the cell retained its integrity throughout.
- The injection system proved to be successful, even if the experiment it was used for did not produce good data. A more appropriate system would exploit this more successfully.

The only significant problem encountered were the steel diffraction peaks which were caused by insufficient collimation. It is therefore recommended that for future measurements the collimation system should be improved to give a smaller diffraction area.

Possibilities for technology transfer to the X-ray Diffraction programme at Daresbury Laboratory

The increased temperature capability available with this experimental setup at the APS could open a new window of research opportunities for the geoscience and material science community. Thus it will be possible to carry out experiments to simulate reactions which occur deep within the Earth's crust or in geothermal centers, and to observe the formation of high temperature hydrothermal phases such as autoclaved cements, in technologically important systems. There is also the possibility of moving into studies in the super critical fluid region. The highest energy X-rays available at

Daresbury Laboratory, from the 6T superconducting wiggler magnet, are far too soft for this work. It will, however, be possible to continue with this work once the new synchrotron, Diamond, is constructed at Daresbury Laboratory. Installation of the current 6T wiggler magnet into Diamond will provide one of the highest energy continuous sources of X-rays in the world. If this were realized then we would be able to embark upon this exciting new field of in-situ material research and establish an internationally commanding position.

Acknowledgments

The calcium silicate research is funded in the UK by the NERC, as part of a CASE studentship between the University of Manchester and Daresbury Laboratory. We would like to thank NERC for funding Sam Shaw for this trip and Daresbury Laboratory for funding Mike Henderson and Simon Clark.

We would like to thank the whole of the GSE-CARS team for the beam time made available for this study and for their excellent technical support, the Daresbury Laboratory for providing the resources for the construction of the hydrothermal equipment and the APS for supplying reliable beam.

Use of the Advanced Photon source was supported by the U.S. Department of Energy, Basic Energy Sciences, Office of Energy Research under Contract No. W-31-109-Eng.-38

References

- 1 A.K. Cheetham and C.F. Mellot, **In Situ Studies of the Sol-Gel Synthesis of Materials**, *Chem. Mater.*, **9** 2269-2279 (1997).
- 2 J.S.O. Evans, R.J. Francis, D. O'Hare, S.J. Price, S.M. Clark, J. Flaherty, J. Gordon, A. Neild and C.C. Tang, **An Apparatus for the study of the Kinetics and Mechanism of Hydrothermal Reactions by In-Situ Energy-Dispersive X-ray Diffraction**, *Rev. Sci. Instr.* **66(3)** 2442-2445 (1994).
- 3 S.M. Clark, A. Neild, T. Rathbone, J. Flaherty, C.C. Tang, J.S.O. Evans, R.J. Francis and D. O'Hare, **Development of large volume reaction cells for kinetic studies using energy-dispersive powder diffraction**, *Nucl. Inst. and Methods*, **B97** 98-101 (1995).
- 4 S.M. Clark, **Energy-dispersive powder diffraction at the SRS**, *Nucl. Inst. and Meth.*, **A276** 381-387 (1989).
- 5 S.M. Clark, **A new energy-dispersive powder diffraction facility at the SRS**, *Nucl. Inst. and Methods*, **A381** 161-168 (1996).
- 6 S. O'Brien, R.J. Francis, S.J. Price, D. O'Hare, S.M. Clark, N. Okazaki and K. Kuroda, **Formation of Silica-Surfactant Mesophases Studied by Real-Time In-Situ X-ray Powder Diffraction**, *Chem. Comm.*, **23** 2423-2424 (1995).
- 7 R.J. Francis, S.J. Price, J.S.O. Evans, S. O'Brien, D. O'Hare and S.M. Clark, **Hydrothermal Synthesis of Microporous Tin Sulfides Studied by Real-Time in-situ Energy-Dispersive X-ray Diffraction**, *Chem. Mater.*, **8(8)** 2102-2108 (1996).
- 8 F. Rey, G. Sankar, J.M. Thomas, P.A. Barret, S.M. Clark, G.N. Greaves and C.R.A. Catlow, **A Synchrotron-based Method for the Study of Crystallisation: The Templated formation of CoALPO-5 Catalyst**, *Chem. Mater.*, **7(8)** 1435-1436 (1995).
- 9 A.T. Davies, G. Sankar, C.R.A. Catlow and S.M. Clark, **Following the crystallisation of microporous solids using EDXRD techniques**, *J. of Physical. Chem.* **101(48)** 10115-10120 (1997).
- 10 S. Komarneni, D.M. Roy and R. Roy, **Al-Substituted tobermorite: show cation exchange**, *Cem. and Concr. Res.* **12(6)** 773-780 (1982)
- 11 G.L. Kalousek, **Crystal chemistry of hydrous calcium silicates: I, substitution of aluminium in the lattice of tobermorite**. *J. Am. Ceram. Soc.* **40(3)** 74-79